Grazing Incidence X-ray Diffraction Measurements of Columnar InAs/GaAs Quantum Dot Structures

Kohki Mukai*, Keita Watanabe, and Yuuta Kimura

Department of Solid State Materials and Engineering, Graduate School of Engineering,

Yokohama National University,

79-5 Tokiwadai, Hodogaya-Ku, Yokohama 240-8501, Japan

*E-mail address: mukai@ynu.ac.jp

The lattice constant distribution inside a columnar InAs/GaAs quantum dot (QD) and its crystal orientation dependence were evaluated by grazing incidence X-ray diffraction (GIXD) measurement. The QDs were grown by stacking Stranski-Krastanow (SK)-type InAs QDs directly in the growth direction with very thin GaAs interval layers. We evaluated the dependence of the in-plane lattice constant on QD height by GIXD measurement using equipment available for laboratories. We found that the lattice constants at the top and bottom of the QDs were almost the same when the height and diameter of the QDs were almost equal. As the number of stacks was increased to grow high QDs, the lattice constant at the QD top became larger in the [1-10] direction than in the [110] direction, but this relationship was reversed at the bottom. We consider that

GIXD measurement with compact equipment will contribute to the swift and efficient development of QD devices.

1. Introduction

Quantum dots (QDs) have been markedly improved in terms of homogeneity, emission wavelength, and quantum efficiency for the application to optical devices. For the development of QD devices for fiber-optic telecommunication and quantum information processing, it is important to control the symmetry of the QD structure, since it affects the polarization characteristics of the devices. For example, the QD semiconductor optical amplifier (QD-SOA) can realize the simultaneous optical amplification of multiple wavelength signals at high speed.[1)] The polarization dependence of amplification by the QD-SOA will be eliminated if a QD structure is symmetric in the propagation direction of light.[2, 3)] The in-plane symmetry of QDs is also important with regard to a QD photon emitter launching entangled photon pairs vertically into a free air space.[4, 5)] The QD form governs the generation processes of two polarized photons, which must be undistinguishable.[6, 7)] The well-known Stranski-Krastanow (SK)-type QD is, however, known to be elongated in the [1-10] direction on a (001) substrate. Recently, a technique of growing closely stacked QDs has led to a columnar QD structure with improved symmetry.[8, 9)]

For the development of structure controllability, the evaluation technique to acquire internal information about QDs has also been paid considerable attention. Cross-sectional scanning tunneling microscopy is a powerful tool for evaluating the QD structure with atomic accuracy,[10)] but it is a destructive method and requires expensive and special sample preparation. Although grazing incidence X-ray diffraction (GIXD) measurement enables the analysis of the internal structure of QDs and is not destructive,

it has been mostly carried out in a synchrotron orbital radiation institution.[11, 12] We have succeeded in performing GIXD measurements on QD structures using equipment available for laboratories.[13] Using an imaging plate (IP) as a detector, we successfully observed the QD-related signals that appeared around a GaAs(220) peak. In this work, the lattice constant distribution inside a columnar InGaAs QD and its crystal orientation dependence were evaluated by GIXD measurement.

2. Experiment

Columnar QDs were grown by stacking SK-type QDs directly in the growth direction.[14] To realize a single columnar form, 0.7 monolayers of InAs QDs were stacked with three-monolayer intervals of GaAs layers after 1.8 monolayers of InAs SK-type base islands had been mounted on a GaAs (001) substrate. We prepared samples where the number of InAs/GaAs stacking units, n, was varied.

The lattice constant inside the samples was evaluated by GIXD measurement. Figure 1 shows the experimental setup. A PANalytical X'Pert PRO MRD system with a four-crystal monochrometor was used as an X-ray source. The incident X-ray beam was a Cu-Kα line and was located at a very small angle ($\approx 0.3°$) close to the total internal reflection angle of the (001) plane surface. We set the sample so that the diffraction may be caused by the (220) and (2-20) planes. We set an IP as near the sample as possible to suppress the attenuation of the diffraction beam due to its propagation through air. Most of the incident beam was reflected at the surface. The diffracted X-ray beam was

irradiated on the IP and detected as two-dimensional information. The diffraction caused by the (220) and (2-20) planes provides the lattice constant in the [110] and [1-10] directions, respectively.

3. Results and Discussion

Figure 2 compares cross-sectional transmission electron microscopy (TEM) images of QD samples observed in the [110] direction. A columnar QD and a multiple wetting layer that originated from the multicyclic growth were observed after they were capped by a GaAs layer. In every sample, the in-plane diameter of the QD is about 15 to 20 nm. The height clearly increases with n. The aspect ratio of the n = 9 sample is almost 1 and the line symmetry of the cross-sectional QD form is good. While the aspect ratio becomes large as n increases, the line symmetry in the vertical direction becomes worse. With the n = 32 sample, the QD form of the upper part is expanded, and some QDs are tilted. The internal crystal distortion distribution must be affected by the change in the QD form.

Figure 3 shows examples of IP images obtained by the GIXD measurements of uncapped columnar QDs. An exposure on a whole IP is shown in Fig. 3(a). A direct beam signal is found at the center, and a (220) diffraction signal is observed on the left. In order to raise the signal intensity, the size of incident x-ray beam was not restricted small. For the reason, the direct beam was broad, especially in the 2θ direction. This affects the shape of diffraction signal. The enlargement of the (220) diffraction signal is shown in Fig.

3(b). For comparison, the (2-20) diffraction signal is shown in Fig. 3(c). The deepest signal is GaAs substrate diffraction, and the upper right signal is QD diffraction. We consider that the difference in the signal intensity between Figs. 3(b) and 3(c) was dependent on the measurement conditions. The value of 2θ is determined on the basis of the most intense position of GaAs diffraction. We can see that the QD signal extends markedly in the 2θ direction, suggesting a large lattice constant variation inside the QD. In addition, the slope of the extended signal differs in the (220) and (2-20) planes. The outgoing angle, α_f, was converted to height, z, by

$$z = \frac{\lambda}{2\pi\alpha_f}\cos^{-1}\frac{\alpha_f}{\alpha_c}, \qquad (1)$$

where α_c is the total internal reflection angle and λ is the X-ray wavelength.[11] Here, we assumed that the interference of X-ray diffraction by the columnar QD with X-ray reflection at the interface of the GaAs substrate and multiple layers was dominant in the IP signal. In order to analyze the IP signal more correctly, it is necessary to take X-ray multiple scattering into consideration with the shape of the uncapped columnar QD. The lattice constant was investigated as a function of QD height using eq. (1). For this purpose, IP data was sliced at every 2θ for the minimum resolution, and the intensity profile was obtained. Then, the main peak values of the profiles were converted to z at every 2θ. Data are missing at some QD heights where the peak was not ascertained owing to a weak and noisy profile.

The lattice constant distributions in various samples are compared in Fig. 4. The data interval depends on the IP signal resolution. Although the resolution of α_f is the same as the resolution of 2θ, the resolution of z is about 1 nm after conversion. Since the height resolution is low compared with the lattice constant resolution, there seems to be two or more symbols at the same height.

Among the four types of samples shown here, a clear difference in the tendency of the lattice constant is observed. With the n = 9 sample, the lattice constant in the [110] direction is smaller than that in the [1-10] direction, and is almost fixed for all heights. With the n = 14 sample, the lattice constants are almost fixed as in the n = 9 sample, but the lattice constants of two directions are very close. On the other hand, with the n = 23 sample, the lattice constant changes from the bottom to the top of the QD. At the bottom, the lattice constant is smaller in the [110] direction than in the [1-10] direction. As the height increases, the relative sizes of the lattice constants in [110] and [1-10] directions are reversed. With the n = 32 sample, the inversion of the relative size of the lattice constants appeared more clearly.

The distribution of the lattice constant must be related to the QD form. In our previous work, we suggested that the polarization dependence of vertical photoluminescence (PL) reveals the anisotropy of the in-plane QD form.[15, 16)] Figure 5 shows the vertical PL spectra of a columnar QD capped by GaAs measured with a linear polarizer. In the measurements, we compared the PL spectra obtained in the most intense polarization direction with those obtained in the perpendicular direction. The most intense polarization direction was [1-10] within the range of ± 10°. We can see in

the figure that the PL intensity in the [1-10] direction relative to that in the [110] direction becomes large as the stacking unit number is increased. The polarization property suggests that the columnar QDs tend to be elongated laterally in the [1-10] direction by increasing the stacking unit number. Note that the direction of the elongation is in agreement with the direction in which the lattice constant expands at the QD top.

Figure 6 shows a schematic of the QD model derived from the results of this study. A side view of a columnar QD and slices at the top and bottom are illustrated. The distribution of the lattice constant within the slices is not considered here. When the height is almost the same as the diameter, the cross section of the QD is almost symmetric but somewhat large in the [1-10] direction. This is probably caused by the form of base SK-type islands. As the height increases, QD inclines and/or spreads toward the [1-10] direction. The in-plane lattice constant must have a causal relationship with the QD form. When the height is small, the lattice constant is somewhat large in the [1-10] direction and is almost fixed for all height because the QD form hardly changes with height. When the QD is high, the lattice constant at the QD top extends in the [1-10] direction, where the QD form is inclined and/or extended. On the other hand, at the QD bottom, we found that the lattice constant is increased in the opposite direction. The result suggests that the lattice constant was redistributed during the increase in QD height.

Let us discuss the reconstruction of the composition and lattice strain during the crystal growth inside the columnar QD. The material redistribution can occur as

interdiffusion and surface migration with strain energy and thermal energy as driving forces.[17, 18] It has been reported that the composition of a QD changes depending on the capping layer.[19] We assume that, in the columnar QD, the strain redistribution at the QD bottom arose following the deformation of the QD upper part so that the net strain in the whole QD is lowered. Further analyses of the internal QD structure will clarify what happens during the growth of a high columnar QD. It should be noted that the lattice constant in this work was derived from the major peak of sliced X-ray diffraction data and does not contain all the information on the slices. Therefore, the detailed in-plane distribution of the lattice constant is still unknown. For example, the distributions of composition and lattice strain will become clear if the X-ray intensity profiles of two orientations are explained simultaneously with a model of the QD structure. Theoretical analysis of PL will support the investigation. These are left for a future study.

4. Conclusions

GIXD measurements were performed with equipment available for laboratories to evaluate the internal structure of columnar InGaAs QDs. Using an IP as a detector, QD-related X-ray diffraction was observed around the GaAs(220) substrate peak. We found that the height dependence of the lattice constant inside the QD was affected by the number of InAs/GaAs stacks in the growth of the columnar QD. When the stacking number was small, the lattice constants at the QD bottom and QD top were almost the

same. However, they became less similar as the stacking number increased. When the height was large, the lattice constant at the QD top was larger in the [1-10] direction than in the [110] direction, but this relationship was reversed at the QD bottom. We expect that GIXD measurement with laboratory equipment will contribute to the swift and efficient development of QD devices.

Acknowledgements

We are grateful to Dr. Mitsuru Sugawara of Fujitsu Laboratories Ltd., for providing the columnar QD samples. This study was supported by Scientific Research (C) of Grants-in-Aid for Scientific Research from Japanese Society for the Promotion of Science and the Iketani Science and Technology Foundation.

References

1) M. Sugawara, T. Akiyama, N. Hatori, Y. Nakata, K. Otsubo, and H. Ebe: Proc. SPIE **4905** (2002) 259.

2) T. Kita, O. Wada, H. Ebe, Y. Nakata, and M. Sugawara: Jpn. J. Appl. Phys. **41** (2002) L1143.

3) K. Kawaguchi, N. Yasuoka, M. Ekawa, H. Ebe, T. Akiyama, M. Sugawara, and Y. Arakawa: Jpn. J. Appl. Phys. **45** (2006) L1244.

4) C. Santori, M. Pelton, G. Solomon, Y. Dale, and Y. Yamamoto: Phys. Rev. Lett. **86** (2001) 1502.

5) T. Miyazawa, K. Takemoto, Y. Sakuma, S. Hirose, T. Usuki, N. Yokoyama, M. Takatsu, and Y. Arakawa: Jpn. J. Appl. Phys. **44** (2005) L620.

6) O. Benson, C. Santori, M. Pelton, and Y. Yamamoto: Phys. Rev. Lett. **84** (2000) 2513.

7) T. M. Stace, G. J. Milburn, and C. H. W. Barnes: Phys. Rev. B **67** (2003) 085317.

8) P. Jayavel, H. Tanaka, T. Kita, O. Wada, H. Ebe, M. Sugawara, J. Tatebayashi, Y. Arakawa, Y. Nakata, and T. Akiyama: Appl. Phys. Lett. **84** (2004) 1820.

9) K. Mukai, K. Watanabe, and K. Nakashima: J. Nanosci. Nanotechnol. **9** (2009) 108.

10) C. H. Lin, W. W. Pai, F. Y. Chang, and H. H. Lin: Appl. Phys. Lett. **90** (2007) 063102.

11) I. Kegel, T. H. Metzger, A. Lorke, J. Peisl, J. Stangl, G. Bauer, and K. Nordlund: Phys. Rev. B **63** (2001) 035318.

12) T. Kaizu, M. Takahasi, K. Yamaguchi, and J. Mizuki: J. Cryst. Growth **301-302** (2007) 248.

13) K. Mukai and Y. Kimura: Jpn. J. Appl. Phys. **48** (2009) 04C147.

14) K. Mukai, Y. Nakata, H. Shoji, M. Sugawara, K. Otsubo, N. Yokoyama, and H. Ishikawa: Electron. Lett. **34** (1998) 1588.

15) K. Mukai and K. Watanabe: e-J. Surf. Sci. Nanotechnol. **7** (2009) 537.

16) K. Mukai and K. Nakashima: Jpn. J. Appl. Phys. **47** (2008) 5057.

17) P. B. Joyce, T. J. Krzyzewski, G. R. Bell, and T. S. Jones: Appl. Phys. Lett. **79** (2001) 3615.

18) K. Mukai and Y. Nakatomi: J. Cryst. Growth **294** (2006) 268.

19) J. M. Uiioa, I. W. D. Drouzas, P. M. Koenraad, D. J. Mowbray, M. J. Steer, H. Y. Liu, and M. Hopkinson: Appl. Phys. Lett. **90** (2007) 213105.

Figure captions

Fig. 1. Schematic of the setup for GIXD measurement.

Fig. 2. Cross-sectional TEM images of the columnar QD; number of stacking units, (a) n = 9, (b) n = 14, and (c) n = 32.

Fig. 3. IP images of n = 32 sample obtained by GIXD measurement; (a) whole IP, (b) (220) diffraction, and (c) (2-20) diffraction.

Fig. 4. Lattice constant as a function of QD height; (a) n = 9, (b) n = 14, (c) n = 23, and (d) n = 32. Results in [1-10] and [110] directions are compared.

Fig. 5. PL spectra perpendicular to the sample surface measured with a linear polarizer at room temperature.

Fig. 6. Schematic of the QD model derived from the results of X-ray diffraction and PL measurements.

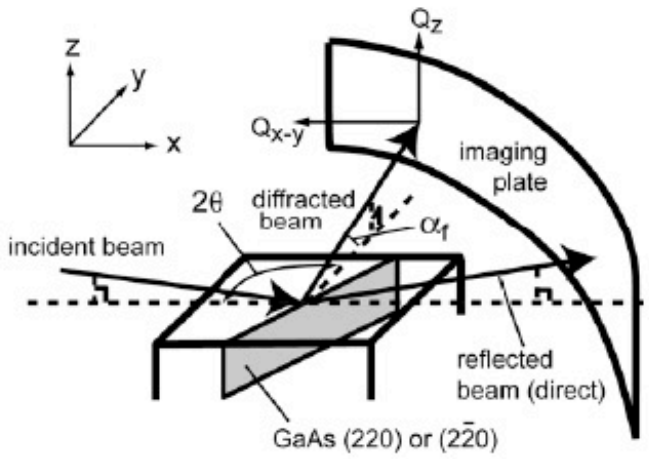

Figure 1: K. Mukai et al.

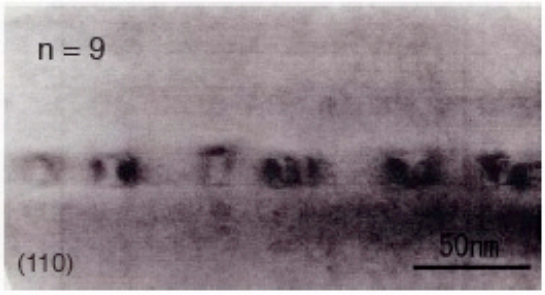

(a)

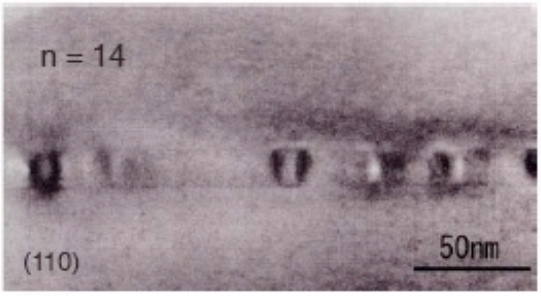

(b)

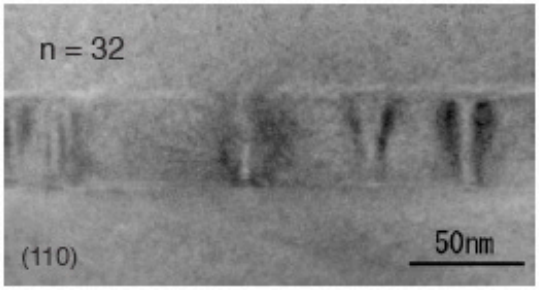

(c)

Figure 2: K. Mukai et al.

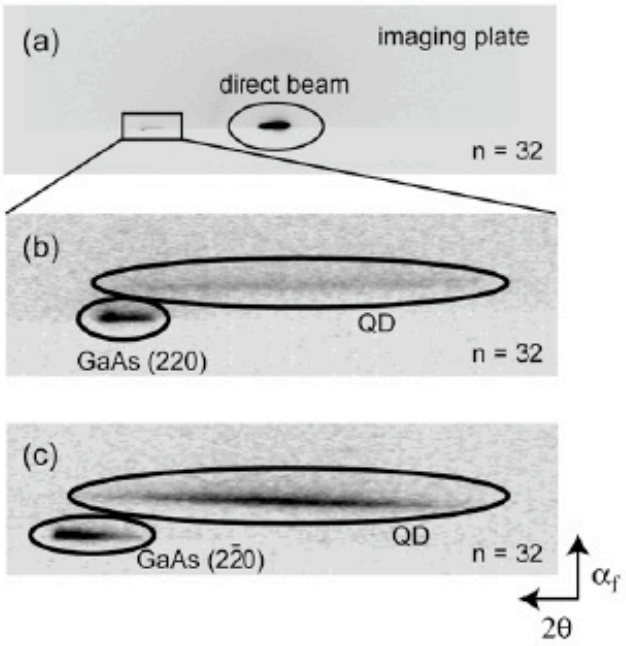

Figure 3: K. Mukai et al.

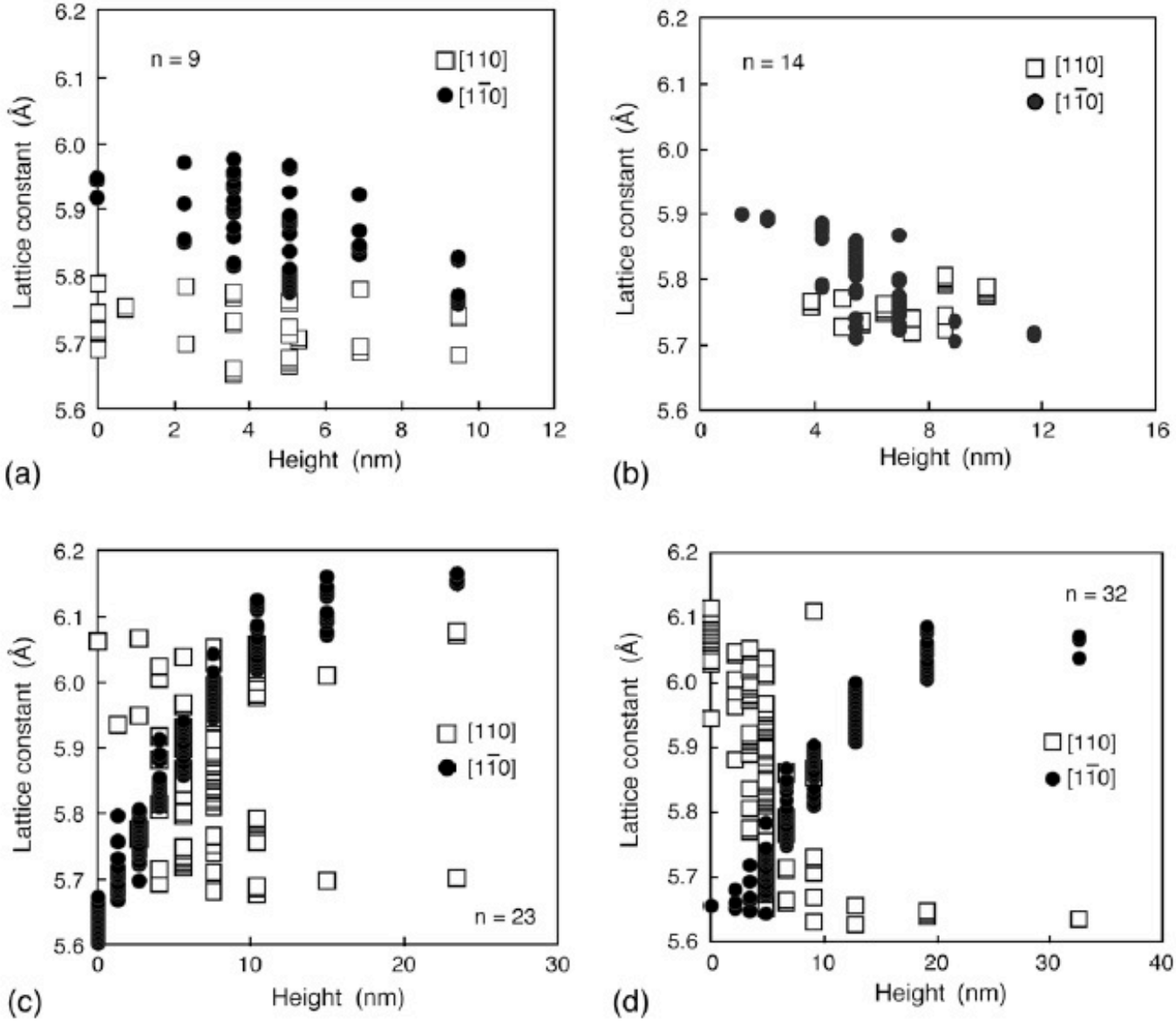

Figure 4: K. Mukai et al.

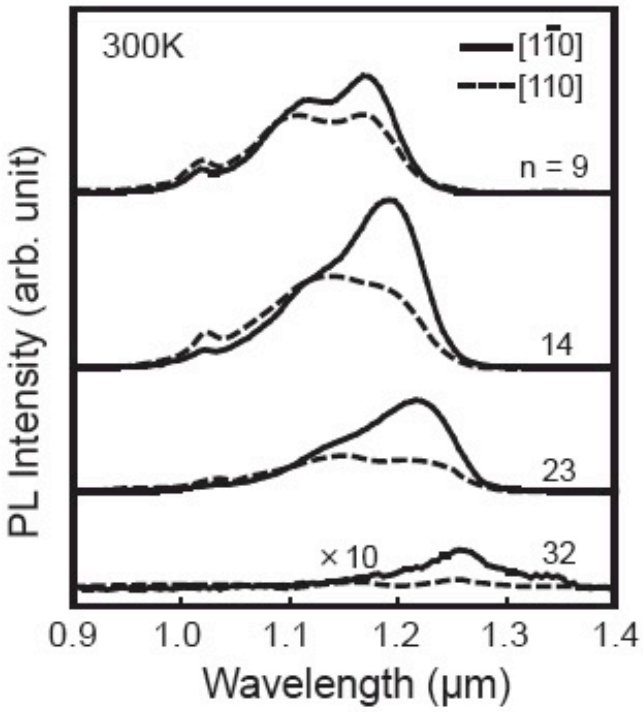

Figure 5: K. Mukai et al.

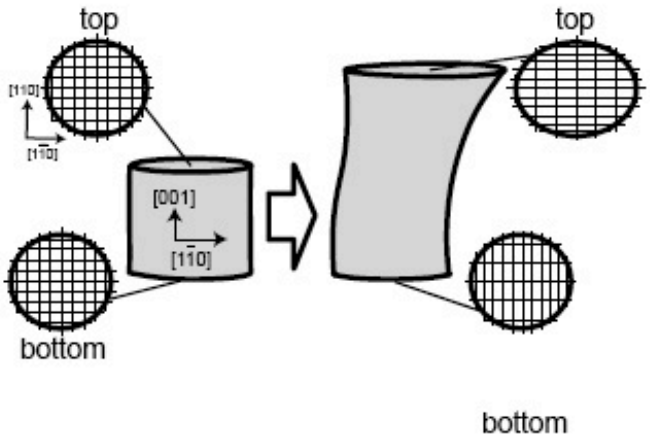

Figure 6: K. Mukai et al.